SEARCHES FOR LEPTON FLAVOUR AND LEPTON NUMBER VIOLATION IN KAON DECAYS

Evgueni Goudzovski
Centre for Cosmology, Particle Physics and Phenomenology,
Catholic University of Louvain, B-1348 Louvain-la-Neuve, Belgium
and
School of Physics and Astronomy, University of Birmingham,
Edgbaston, Birmingham, B15 2TT, United Kingdom

Searches for lepton flavour and lepton number violation in kaon decays by the NA48/2 and NA62 experiments at CERN are presented. A new measurement of the helicity suppressed ratio of charged kaon leptonic decay rates $R_K = \Gamma(K_{e2})/\Gamma(K_{\mu 2})$ to sub-percent relative precision is discussed. An improved upper limit on the lepton number violating $K^\pm \to \pi^\mp \mu^\pm \mu^\pm$ decay rate is also presented.

1 Introduction

In the Standard Model (SM) the decays of pseudoscalar mesons to light leptons are helicity suppressed. In particular, the SM width of $P^\pm \to \ell^\pm \nu$ decays with $P = \pi, K, D, B$ (denoted $P_{\ell 2}$ in the following) is

$$\Gamma^{\rm SM}(P^\pm \to \ell^\pm \nu) = \frac{G_F^2 M_P M_\ell^2}{8\pi}\left(1 - \frac{M_\ell^2}{M_P^2}\right)^2 f_P^2 |V_{qq'}|^2, \tag{1}$$

where G_F is the Fermi constant, M_P and M_ℓ are meson and lepton masses, f_P is the decay constant, and $V_{qq'}$ is the corresponding Cabibbo-Kobayashi-Maskawa matrix element. Although the SM predictions for the $P_{\ell 2}$ decay rates are limited by hadronic uncertainties, their specific ratios do not depend on f_P and can be computed very precisely. In particular, the SM prediction for the ratio $R_K = \Gamma(K_{e2})/\Gamma(K_{\mu 2})$ of kaon leptonic decay widths inclusive of internal bremsstrahlung (IB) radiation is [1]

$$R_K^{\rm SM} = \left(\frac{M_e}{M_\mu}\right)^2 \left(\frac{M_K^2 - M_e^2}{M_K^2 - M_\mu^2}\right)^2 (1 + \delta R_{\rm QED}) = (2.477 \pm 0.001) \times 10^{-5}, \tag{2}$$

where $\delta R_{\rm QED} = (-3.79 \pm 0.04)\%$ is an electromagnetic correction due to the IB and structure-dependent effects.

Within certain two Higgs doublet models (2HDM of type II), including the minimal supersymmetric model (MSSM), R_K is sensitive to lepton flavour violating (LFV) effects appearing at the one-loop level via the charged Higgs boson ($H^\pm$) exchange [2,3], representing a unique probe into mixing in the right-handed slepton sector [4]. The dominant contribution due to the LFV

coupling of the $H^{\pm}$ is

$$R_K^{\rm LFV} \simeq R_K^{\rm SM}\left[1+\left(\frac{M_K}{M_H}\right)^4\left(\frac{M_\tau}{M_e}\right)^2|\Delta_R^{31}|^2\tan^6\beta\right], \quad (3)$$

where $\tan\beta$ is the ratio of the two Higgs vacuum expectation values, and $|\Delta_R^{31}|$ is the mixing parameter between the superpartners of the right-handed leptons, which can reach $\sim 10^{-3}$. This can enhance R_K by $\mathcal{O}(1\%)$ without contradicting any experimental constraints known at present, including upper bounds on the LFV decays $\tau \to eX$ with $X = \eta, \gamma, \mu\bar{\mu}$. On the other hand, R_K is sensitive to the neutrino mixing parameters within the SM extension involving a fourth generation [5].

The first measurements of R_K were performed in the 1970s [6,7,8], while the current PDG world average [9] is based on a more precise recent result [10] $R_K = (2.493 \pm 0.031) \times 10^{-5}$. A new measurement of R_K based on a part of a dedicated data sample collected by the NA62 experiment at CERN in 2007 is reported here: the analyzed K_{e2} sample is ~ 4 times larger than the total world sample, allowing the first measurement of R_K with a relative precision below 1%.

The decay $K^{\pm} \to \pi^{\mp}\mu^{\pm}\mu^{\pm}$ violating lepton number by two units can proceed via a neutrino exchange if the neutrino is a Majorana particle, consequently the experimental limits on this decay provide constraints on the effective Majorana neutrino mass $\langle m_{\mu\mu}\rangle$ [11]. This decay has also been studied in the context of supersymmetric models with R-parity violation [12]. The best previous upper limit on the decay rate was based on a special data set collected by the BNL E865 experiment in 1997 [13]. The sample of $\pi\mu\mu$ triggers collected by the NA48/2 experiment at CERN during the 2003–04 data taking is about 8 times larger than the E865 one, which allows improving the upper limit significantly.

2 Beam and detector

The NA48/2 and NA62 (phase I) experiments at CERN took data in 2003–04 and 2007–08, respectively, using the same kaon beamline and experimental setup [14]. The trigger logic was optimized to detect direct CP violating charge asymmetries in $K^{\pm}$ decays in 2003–04 [15], and for the $K_{e2}/K_{\mu 2}$ ratio measurement in 2007–08. The beam line is capable of delivering simultaneous unseparated K^+ and K^- beams derived from the 400 GeV/c primary proton beam extracted from the CERN SPS. Central values of kaon momentum of 60 GeV/c (both K^+ and K^- beams) and 74 GeV/c (K^+ beam only), with a narrow momentum band, were used for collection of the main data samples by the NA48/2 and NA62 experiments, correspondingly.

The fiducial decay region is contained in a 114 m long cylindrical vacuum tank. With $\sim 10^{12}$ primary protons incident on the target per SPS pulse of 4.8 s duration, the typical secondary beam flux at the entrance to the decay volume is 10^7 to 10^8 particles per pulse, of which about 5% are kaons, while pions constitute the dominant component. The transverse size of the beams within the decay volume is below 1 cm (rms), and their angular divergence is negligible.

Among the subdetectors located downstream the decay volume, a magnetic spectrometer, a plastic scintillator hodoscope (HOD), a liquid krypton electromagnetic calorimeter (LKr) and a muon veto counter (MUV) are principal for the present measurements. The spectrometer, used to detect charged products of kaon decays, is composed of four drift chambers (DCHs) and a dipole magnet. The HOD producing fast trigger signals consists of two planes of strip-shaped counters. The LKr, used for particle identification and as a veto, is an almost homogeneous ionization chamber, $27X_0$ deep, segmented transversally into 13,248 cells (2×2 cm^2 each), and with no longitudinal segmentation. The MUV is composed of three planes of plastic scintillator strips read out by photomultipliers at both ends. A beam pipe traversing the centres of the

detectors allows undecayed beam particles and muons from decays of beam pions to continue their path in vacuum.

3 Search for lepton flavour violation

The precision measurement of $R_K = \Gamma(K_{e2})/\Gamma(K_{\mu 2})$ is based on the NA62 2007 data sample. The measurement method is based on counting the numbers of reconstructed K_{e2} and $K_{\mu 2}$ candidates collected concurrently. Consequently the result does not rely on kaon flux measurement, and several systematic effects (e.g. due to reconstruction and trigger efficiencies, time-dependent effects) cancel to first order. To take into account the significant dependence of signal acceptance and background level on lepton momentum, the measurement is performed independently in bins of this observable: 10 bins covering a lepton momentum range of $(13; 65)$ GeV/c are used. The ratio R_K in each bin is computed as

$$R_K = \frac{1}{D} \cdot \frac{N(K_{e2}) - N_{\rm B}(K_{e2})}{N(K_{\mu 2}) - N_{\rm B}(K_{\mu 2})} \cdot \frac{A(K_{\mu 2})}{A(K_{e2})} \cdot \frac{f_\mu \times \epsilon(K_{\mu 2})}{f_e \times \epsilon(K_{e2})} \cdot \frac{1}{f_{\rm LKr}}, \tag{4}$$

where $N(K_{\ell 2})$ are the numbers of selected $K_{\ell 2}$ candidates ($\ell = e, \mu$), $N_{\rm B}(K_{\ell 2})$ are numbers of background events, $A(K_{\mu 2})/A(K_{e2})$ is the geometric acceptance correction, f_ℓ are efficiencies of e/μ identification, $\epsilon(K_{\ell 2})$ are trigger efficiencies, $f_{\rm LKr}$ is the global efficiency of the LKr readout, and $D = 150$ is the downscaling factor of the $K_{\mu 2}$ trigger.

A detailed Monte Carlo (MC) simulation including beam line optics, full detector geometry and material description, stray magnetic fields, local inefficiencies of DCH wires, and time variations of the above throughout the running period, is used to evaluate the acceptance correction $A(K_{\mu 2})/A(K_{e2})$ and the geometric parts of the acceptances for background processes entering the computation of $N_B(K_{\ell 2})$. Simulations are used to a limited extent only: particle identification, trigger and readout efficiencies are measured directly.

Due to the topological similarity of K_{e2} and $K_{\mu 2}$ decays, a large part of the selection conditions is common for both decays: (1) exactly one reconstructed positively charged particle compatible with originating from a beam K decay; (2) its momentum 13 GeV/c $< p <$ 65 GeV/c (the lower limit is due to the 10 GeV LKr energy deposit trigger requirement); (3) extrapolated track impact points in subdetectors are within their geometrical acceptances; (4) no LKr energy deposition clusters with energy $E > 2$ GeV not associated to the track, to suppress background from other kaon decays; (5) distance between the charged track and the nominal kaon beam axis CDA < 3 cm, and decay vertex longitudinal position within the nominal decay volume.

The following two principal selection criteria are different for the K_{e2} and $K_{\mu 2}$ decays. $K_{\ell 2}$ kinematic identification is based on the reconstructed squared missing mass assuming the track to be a positron or a muon: $M^2_{\rm miss}(\ell) = (P_K - P_\ell)^2$, where P_K and P_ℓ ($\ell = e, \mu$) are the four-momenta of the kaon (average beam momentum assumed) and the lepton (positron or muon mass assumed). A selection condition $-M_1^2 < M^2_{\rm miss}(\ell) < M_2^2$ is applied to select $K_{\ell 2}$ candidates, where M_1^2 varies between 0.013 and 0.016 (GeV/c^2)^2 and M_2^2 between 0.010 and 0.013 (GeV/c^2)^2 across the lepton momentum bins, depending on $M^2_{\rm miss}(\ell)$ resolution. Particle identification is based on the ratio E/p of track energy deposit in the LKr calorimeter to its momentum measured by the spectrometer. Particles with $0.95 < E/p < 1.1$ ($E/p < 0.85$) are identified as positrons (muons).

Kinematic separation of K_{e2} from $K_{\mu 2}$ decays is achievable at low lepton momentum only ($p < 35$ GeV/c). At high lepton momentum, the $K_{\mu 2}$ decay with a mis-identified muon ($E/p > 0.95$) is the largest background source. The dominant process leading to mis-identification of the muon as a positron is 'catastrophic' bremsstrahlung in or in front of the LKr leading to significant energy deposit in the LKr. Mis-identification due to accidental LKr clusters associated with

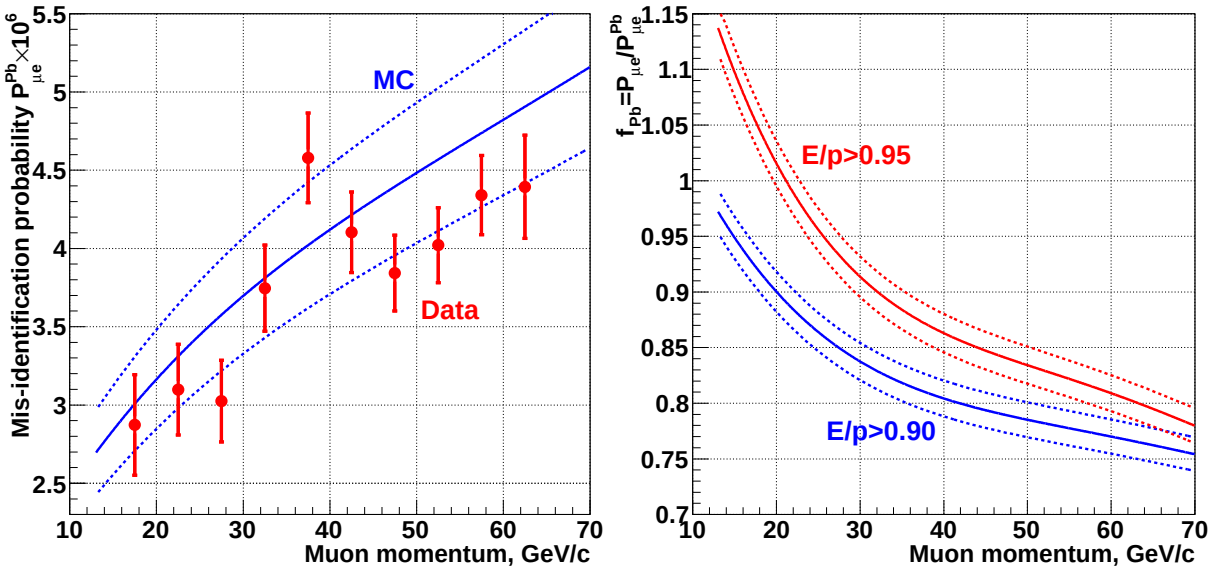

Figure 1: Left: Mis-identification probability for muons traversing the lead wall, $P^{\rm Pb}_{\mu e}$, for $(E/p)_{\rm min} = 0.95$ as a function of momentum: measurement (solid circles with error bars) and simulation (solid line). Right: Correction factors $f_{\rm Pb} = P_{\mu e}/P^{\rm Pb}_{\mu e}$ for the considered values of $(E/p)_{\rm min}$, as evaluated with simulation. Dotted lines in both plots indicate the estimated systematic uncertainties of the simulation.

the muon track is negligible, as concluded from a study of the sidebands of track-cluster time difference and distance distributions.

The muon mis-identification probability $P_{\mu e}$ has been measured as a function of momentum. To collect a muon sample free from the typical $\sim 10^{-4}$ positron contamination due to $\mu \to e$ decays, a $9.2X_0$ thick lead (Pb) wall covering $\sim 20\%$ of the geometric acceptance was installed approximately 1.2 m in front of the LKr calorimeter (between the two HOD planes) during a period of data taking. The component from positrons which traverse the Pb wall and are mis-identified as muons from $K_{\mu 2}$ decay with $p > 30$ GeV/c and $E/p > 0.95$ is suppressed down to a negligible level ($\sim 10^{-8}$) by energy losses in the Pb.

However, muon passage through the Pb wall affects the measured $P^{\rm Pb}_{\mu e}$ via two principal effects: 1) ionization energy loss in Pb decreases $P_{\mu e}$ and dominates at low momentum; 2) bremsstrahlung in Pb increases $P_{\mu e}$ and dominates at high momentum. To evaluate the correction factor $f_{\rm Pb} = P_{\mu e}/P^{\rm Pb}_{\mu e}$, a dedicated MC simulation based on Geant4 (version 9.2) has been developed to describe the propagation of muons downstream from the last DCH, involving all electromagnetic processes including muon bremsstrahlung [16].

The measurements of $P^{\rm Pb}_{\mu e}$ in momentum bins compared with the results of the MC simulation and the correction factors $f_{\rm Pb}$ obtained from simulation, along with the estimated systematic uncertainties of the simulated values, are shown in Fig. 1. The relative systematic uncertainties on $P_{\mu e}$ and $P^{\rm Pb}_{\mu e}$ obtained by simulation have been estimated to be 10%, and are mainly due to the simulation of cluster reconstruction and energy calibration. However the error of the ratio $f_{\rm Pb} = P_{\mu e}/P^{\rm Pb}_{\mu e}$ is significantly smaller ($\delta f_{\rm Pb}/f_{\rm Pb} = 2\%$) due to cancellation of the main systematic effects. The measured $P^{\rm Pb}_{\mu e}$ is in agreement with the simulation within their uncertainties.

The $K_{\mu 2}$ background contamination integrated over lepton momentum has been computed to be $(6.11 \pm 0.22)\%$ using the measured $P^{\rm Pb}_{\mu e}$ corrected by $f_{\rm Pb}$. The quoted error is due to the limited size of the data sample used to measure $P^{\rm Pb}_{\mu e}$ (0.16%), the uncertainty $\delta f_{\rm Pb}$ (0.12%), and the model-dependence of the correction for the $M^2_{\rm miss}(e)$ vs E/p correlation (0.08%).

R_K is defined to be fully inclusive of internal bremsstrahlung (IB) radiation [1]. The structure-dependent (SD) $K^+ \to e^+\nu\gamma$ process [17,18] may lead to a K_{e2} signature if the positron is energetic and the photon is undetected. In particular, the $\rm SD^+$ component with positive photon helicity

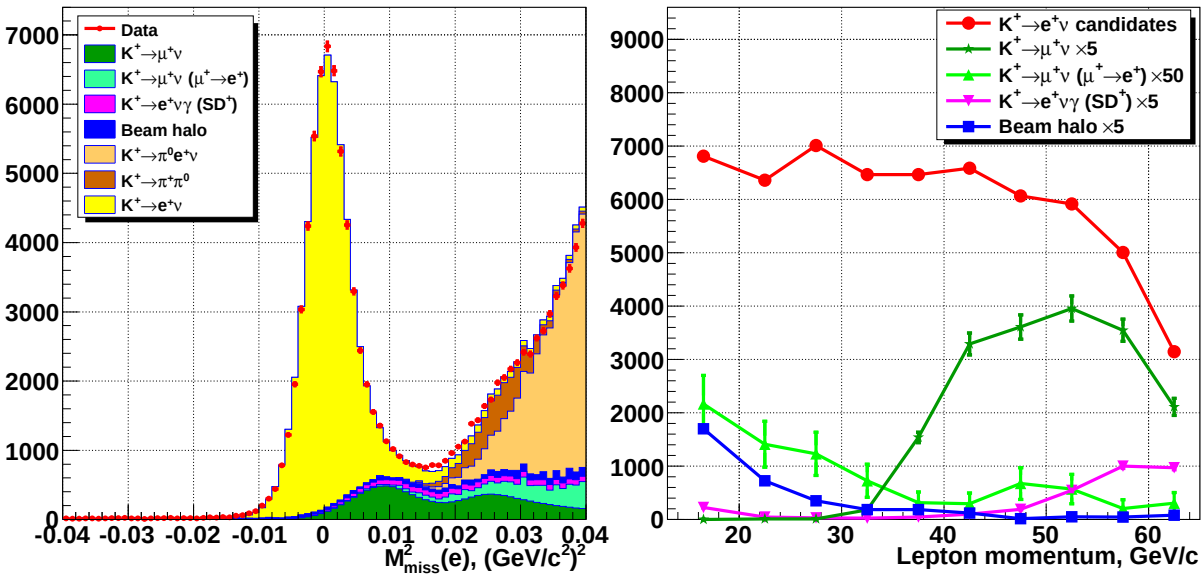

Figure 2: Left: Reconstructed squared missing mass $M^2_{\rm miss}(e)$ distribution of the K_{e2} candidates compared with the sum of normalised estimated signal and background components. Right: Lepton momentum distributions of the K_{e2} candidates and the dominant backgrounds; the backgrounds are scaled for visibility.

Table 1: Summary of backgrounds in the K_{e2} sample.

Source	$N_B/N(K_{e2})$
$K_{\mu 2}$	$(6.11 \pm 0.22)\%$
$K_{\mu 2}(\mu \to e)$	$(0.27 \pm 0.04)\%$
$K^+ \to e^+\nu\gamma$ (SD$^+$)	$(1.07 \pm 0.05)\%$
$K^+ \to \pi^0 e^+\nu$	$(0.05 \pm 0.03)\%$
$K^+ \to \pi^+\pi^0$	$(0.05 \pm 0.03)\%$
Beam halo	$(1.16 \pm 0.06)\%$
Total	$(8.71 \pm 0.24)\%$

peaks at high positron momentum in the K^+ rest frame ($E^*_e \approx M_K/2$) and has a similar branching ratio to K_{e2}. The background due to $K^+ \to e^+\nu\gamma$ (SD$^-$) decay with negative photon helicity peaking at $E^*_e \approx M_K/4$ and the interference between the IB and SD processes are negligible. The SD$^+$ background contribution has been estimated by MC simulation as $(1.07 \pm 0.05)\%$, using a recent measurement of the $K^+ \to e^+\nu\gamma$ (SD$^+$) differential decay rate [10]. The quoted uncertainty is due to the limited precision on the form factors and decay rate, and is therefore correlated between lepton momentum bins.

The beam halo background in the K_{e2} sample induced by halo muons (undergoing $\mu \to e$ decay in flight or mis-identified) is measured using a data-driven method, by reconstructing K^+_{e2} candidates from a control K^- data sample collected with the K^+ beam dumped, to be $(1.16 \pm 0.06)\%$. Background rate and kinematical distribution are qualitatively reproduced by a halo simulation. The uncertainty is due to the limited size of the control sample. The beam halo is the only significant background source in the $K_{\mu 2}$ sample. Its contribution is mainly at low muon momentum, and has been measured to be $(0.38 \pm 0.01)\%$ using the same technique as for the K_{e2} sample.

The numbers of selected K_{e2} and $K_{\mu 2}$ candidates are 59813 and 1.803×10^7, respectively (the latter samples has been pre-scaled by a factor of 150 at the trigger level). Backgrounds in the K_{e2} sample integrated over lepton momentum are summarised in Table 1: the total background contamination is $(8.71 \pm 0.24)\%$, and its uncertainty is smaller than the relative statistical

Table 2: Summary of the uncertainties on R_K.

Source	$\delta R_K \times 10^5$
Statistical	0.011
$K_{\mu 2}$ background	0.005
$K^+ \to e^+\nu\gamma$ (SD^+) background	0.001
$K^+ \to \pi^0 e^+\nu$, $K^+ \to \pi^+\pi^0$ backgrounds	0.001
Beam halo background	0.001
Helium purity	0.003
Acceptance correction	0.002
Spectrometer alignment	0.001
Positron identification efficiency	0.001
1-track trigger efficiency	0.002
LKr readout inefficiency	0.001
Total systematic	0.007
Total	0.013

uncertainty of 0.43%. The $M^2_{\mathrm{miss}}(e)$ and lepton momentum distributions of K_{e2} candidates and backgrounds are shown in Fig. 2.

The ratio of geometric acceptances $A(K_{\mu 2})/A(K_{e2})$ in each lepton momentum bin has been evaluated with MC simulation. The radiative $K^+ \to e^+\nu\gamma$ (IB) process, which is responsible for the loss of about 5% of the K_{e2} acceptance by increasing the reconstructed $M^2_{\mathrm{miss}}(e)$, is taken into account following [17], with higher order corrections according to [19,20].

The acceptance correction is strongly influenced by bremsstrahlung suffered by the positron in the material upstream of the spectrometer magnet (Kevlar window, helium, DCHs). This results in an almost momentum-independent loss of K_{e2} acceptance of about 6%, mainly by increasing the reconstructed $M^2_{\mathrm{miss}}(e)$. The relevant material thickness has been measured by studying the spectra and rates of bremsstrahlung photons produced by low intensity 25 GeV/c and 40 GeV/c electron and positron beams steered into the DCH acceptance, using special data samples collected in the same setup by the NA48/2 experiment in 2004 and 2006. The material thickness during the 2007 run has been estimated to be $(1.56 \pm 0.03)\% X_0$, where the quoted uncertainty is dominated by the limited knowledge of helium purity in the spectrometer tank.

A χ^2 fit to the measurements of R_K in the 10 lepton momentum bins has been performed, taking into account the bin-to-bin correlations between the systematic errors. The uncertainties of the combined result are summarized in Table 2. To validate the assigned systematic uncertainties, extensive stability checks have been performed in bins of kinematic variables and by varying selection criteria and analysis procedures. The fit result is [21]

$$R_K = (2.487 \pm 0.011_{\mathrm{stat.}} \pm 0.007_{\mathrm{syst.}}) \times 10^{-5} = (2.487 \pm 0.013) \times 10^{-5}, \qquad (5)$$

with $\chi^2/\mathrm{ndf} = 3.6/9$. The individual measurements with their statistical and total uncertainties, the combined NA62 result, and the new world average are presented in Fig. 3.

4 Search for lepton number violation

The $K^\pm \to \pi^\mp\mu^\pm\mu^\pm$ decay has been searched for using the NA48/2 2003–04 data sample, normalizing to the abundant $K^\pm \to \pi^\pm\pi^+\pi^-$ normalization channel (denoted $K_{3\pi}$ below). Three-track vertices (compatible with either $K^\pm \to \pi\mu\mu$ or $K_{3\pi}$ decay topology) are reconstructed by extrapolation of track segments from the spectrometer upstream into the decay volume, taking into account the measured Earth's magnetic field, stray fields due to magnetization of the

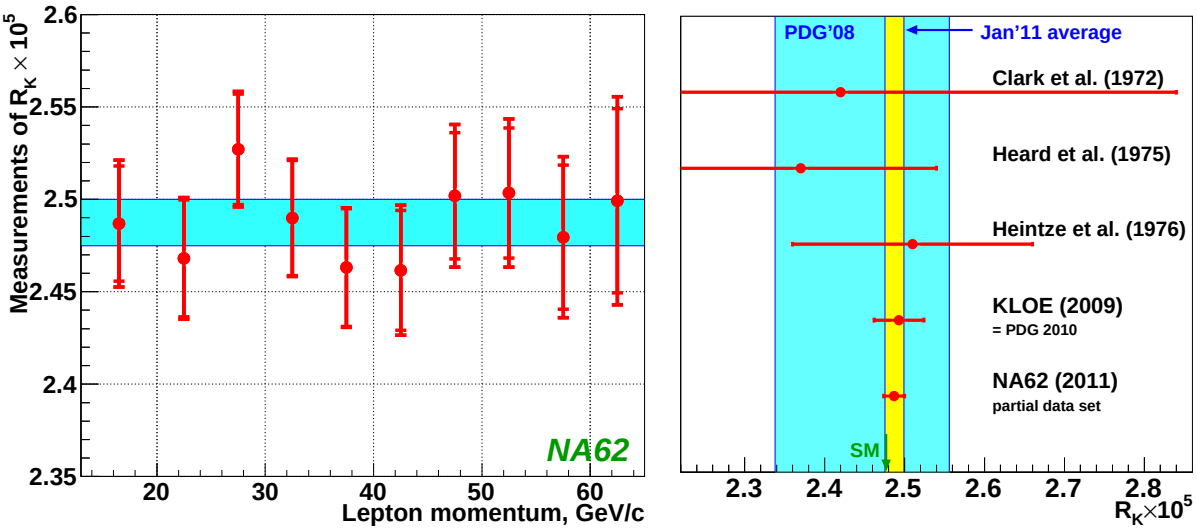

Figure 3: Left: Measurements of R_K in lepton momentum bins with their uncorrelated statistical uncertainties and the partially correlated total uncertainties; the average R_K and its total uncertainty are indicated by a band. Right: The new world average including the present result.

vacuum tank, and multiple scattering. The vertex is required to have no significant missing momentum, and to be composed of one $\pi^\pm$ candidate (with the ratio of energy deposition in the LKr calorimeter to momentum measured by the spectrometer $E/p < 0.95$, which suppresses electrons, and no in-time associated hits in the MUV), and a pair of $\mu^\pm$ candidates (with $E/p < 0.2$ and associated signal in the MUV). The muon identification efficiency has been measured to be above 98% for $p > 10$ GeV/c, and above 99% for $p > 15$ GeV/c.

The invariant mass spectra of the reconstructed $\pi^\pm\mu^\pm\mu^\mp$ and $\pi^\mp\mu^\pm\mu^\pm$ candidates are presented in Fig. 4. The observed flavour changing neutral current $K^\pm \to \pi^\pm\mu^\pm\mu^\mp$ decay (3120 candidates with a background of 3.3%) has been studied separately [22]. In the mass spectrum with same sign muons, corresponding to the lepton number violating signature, 52 events are observed in the signal region $|M_{\pi\mu\mu} - M_K| < 8$ MeV/c^2. The background comes from the $K_{3\pi}$ decay, and has been estimated by MC simulation to be (52.6 ± 19.8) events. The quoted uncertainty is systematic due to the limited precision of MC description of the high-mass region, and has been estimated from the level of data/MC agreement in the control mass region of (465; 485) MeV/c^2. This background estimate has been cross-checked by fitting the mass spectrum in the region between 460 and 520 MeV/c^2, excluding the signal region between 485 and 502 MeV/c^2, with an empirical function similar to that used in the E865 analysis [13] using the maximum likelihood estimator and assuming a Poisson probability density in each mass bin.

The Feldman-Cousins method [23] is employed for confidence interval evaluation; the systematic uncertainty of the background estimate is taken into account. Conservatively assuming the expected background to be $52.6 - 19.8 = 32.8$ events to take into account its uncertainty, this translates into an upper limit of 32.2 signal events at 90% CL. The geometrical acceptance is conservatively assumed to be the smallest of those averaged over the $K^\pm \to \pi^\pm\mu^\pm\mu^\mp$ and $K_{3\pi}$ samples ($A_{\pi\mu\mu} = 15.4\%$ and $A_{3\pi} = 22.2\%$). This leads to an upper limit [22] of $\mathrm{BR}(K^\pm \to \pi^\mp\mu^\pm\mu^\pm) < 1.1 \times 10^{-9}$ at 90% CL, which improves the best previous limit [13] by almost a factor of 3.

5 Conclusions

The most precise measurement of lepton flavour violation parameter R_K has been performed: $R_K = (2.487 \pm 0.013) \times 10^{-5}$ is consistent with the SM expectation, and can be used to constrain

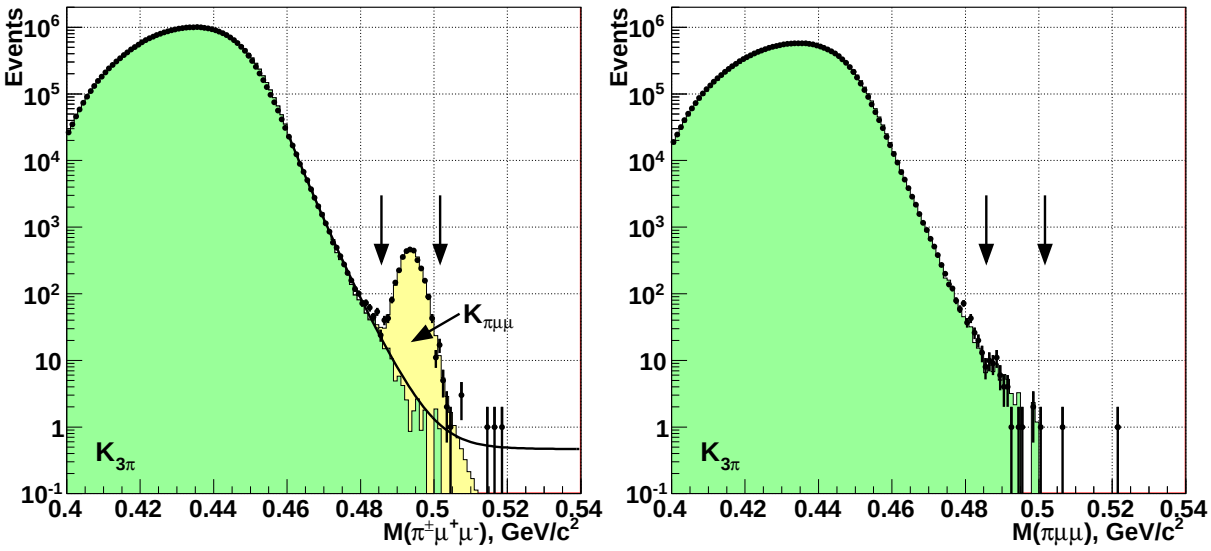

Figure 4: Reconstructed $M_{\pi\mu\mu}$ spectra for candidates with different (left) and same sign (right) muons: data (dots), $K_{3\pi}$ and $K_{\pi\mu\mu}$ MC simulations (filled areas); fit to background using the empirical parameterization as explained in the text (solid line). The signal region is indicated with arrows.

multi-Higgs [2] and fourth generation [5] new physics scenarios. An improved upper limit of 1.1×10^{-9} for the branching fraction of the lepton number violating $K^{\pm} \to \pi^{\mp}\mu^{\pm}\mu^{\pm}$ decay has been established.

References

1. V. Cirigliano and I. Rosell, *Phys. Rev. Lett.* **99**, 231801 (2007).
2. A. Masiero, P. Paradisi and R. Petronzio, *Phys. Rev.* D **74**, 011701 (2006).
3. A. Masiero, P. Paradisi and R. Petronzio, *JHEP* **0811**, 042 (2008).
4. J. Ellis, S. Lola and M. Raidal, *Nucl. Phys.* B **812**, 128 (2009).
5. H. Lacker and A. Menzel, *JHEP* **1007**, 006 (2010).
6. A.G. Clark *et al*, *Phys. Rev. Lett.* **29**, 1274 (1972).
7. K.S. Heard *et al*, *Phys. Lett.* B **55**, 327 (1975).
8. J. Heintze *et al*, *Phys. Lett.* B **60**, 302 (1976).
9. K. Nakamura *et al* (PDG), *J. Phys.* G **37**, 075021 (2010).
10. F. Ambrosino *et al*, *Eur. Phys. J.* C **64**, 627 (2009); ibid. C **65**, 703 (2010).
11. K. Zuber, *Phys. Lett.* B **479**, 33 (2000).
12. L.S. Littenberg and R. Shrock, *Phys. Lett.* B **491**, 285 (2000).
13. R. Appel *et al*, *Phys. Rev. Lett.* **85**, 2877 (2000).
14. V. Fanti *et al*, *Nucl. Instrum. Methods* A **574**, 433 (2007).
15. J.R. Batley *et al*, *Eur. Phys. J.* C **52**, 875 (2007).
16. S.R. Kelner, R.P. Kokoulin and A.A. Petrukhin, *Phys. Atom. Nucl.* **60**, 576 (1997).
17. J. Bijnens, G. Ecker and J. Gasser, *Nucl. Phys.* B **396**, 81 (1993).
18. C.H. Chen, C.Q. Geng and C.C. Lih, *Phys. Rev.* D **77**, 014004 (2008).
19. S. Weinberg, *Phys. Rev.* **140**, B516 (1965).
20. C. Gatti, *Eur. Phys. J.* C **45**, 417 (2006).
21. C. Lazzeroni *et al*, *Phys. Lett.* B **698**, 105 (2011).
22. J.R. Batley *et al*, *Phys. Lett.* B **697**, 107 (2011).
23. G.J. Feldman and R.D. Cousins, *Rhys. Rev.* D **57**, 3873 (1998).